REPORT DOCUMENTATION PAGE

Form Approved
OMB No. 0704-0188

Public reporting burden for this collection of information is estimated to average 1 hour per response, including the time for reviewing instructions, searching existing data sources, gathering and maintaining the data needed, and completing and reviewing the collection of information. Send comments regarding this burden estimate or any other aspect of this collection of information, including suggestions for reducing this burden, to Washington Headquarters Services, Directorate for Information Operations and Reports, 1215 Jefferson Davis Highway, Suite 1204, Arlington, VA 22202-4302, and to the Office of Management and Budget, Paperwork Reduction Project (0704-0188), Washington, DC 20503.

1. AGENCY USE ONLY (Leave blank)	2. REPORT DATE	3. REPORT TYPE AND DATES COVERED
	2/5/96	Final Report 4/1/93 - 12/31/95

4. TITLE AND SUBTITLE
Heterodyning Single-Photon Pairs

5. FUNDING NUMBERS
N00014-93-1-0547

6. AUTHOR(S)
Prof. Malvin Teich

7. PERFORMING ORGANIZATION NAME(S) AND ADDRESS(ES)
Columbia University
Columbia Radiation Laboratory
530 W. 120th St. Rm 1001, MC8903
New York, NY 10027

8. PERFORMING ORGANIZATION REPORT NUMBER
N00014-93-1-0547

9. SPONSORING/MONITORING AGENCY NAME(S) AND ADDRESS(ES)
Office of Naval Research
800 North Quincy Street
Arlington, VA 22217-5660

10. SPONSORING/MONITORING AGENCY REPORT NUMBER
N00014-93-1-0547

11. SUPPLEMENTARY NOTES
The view, opinions and/or findings contained in this report are those of the author(s) and should not be construed as an official Department of the Army position, policy, or decision, unless so designated by other documentation.

12a. DISTRIBUTION/AVAILABILITY STATEMENT
Approved for public release; distribution unlimited.

12b. DISTRIBUTION CODE

19960703 056

13. ABSTRACT (Max

Abstract: We have obtained theoretical and experimental second- and fourth-order interference patterns for entangled photons of different colors entering single and dual Mach-Zehnder interferometers (MZIs) in which dispersive elements have been deliberately placed.[1,2] Entangled-photon pairs are a form of nonclassical light. We have observed the interference of entangled photons of different colors, in both second- and fourth-order, using coincidence detection, by sweeping the path-length difference in an interferometer (or two spatially separated interferometers). The entangled photons are created by pumping a KD*P parametric-downconverter crystal with a krypton-ion laser beam at 413 nm, creating photon pairs with center wavelengths in the vicinity of 830 nm. The coherence properties and photon statistics of this nonclassical source of light were determined. Although photon wavepackets are generally broadened, as well as delayed, by passage through dispersive optical elements, coincidence measurements made with entangled photon pairs can be free of such broadening. This occurs for materials with particular dispersive behavior, as well as when the dispersion is balanced in both arms. This nonlocal behavior arises from the entanglement in the frequencies of the downconverted pair photons. We have shown that pump-frequency oscillations are present in the coincidence rate patterns for arbitrarily long path-length-difference times, confirming the robustness of this nonlocal phenomenon in the presence of dispersion. The difference-frequency oscillations, which correspond to heterodyning single-photon pairs, are also robust in the presence of dispersion, though they decay for large path-length-differences. Potential areas of applicability of twin photon beams range from photonics to visual science to computer science. Three examples are: (1) the direct measurement of the gain fluctuations in fiber amplifiers and avalanche photodiodes; (2) the direct determination of neural noise in a visual photoreceptor; and (3) key sharing in a quantum-cryptographic system for secure communications.

:T TERM

OF PAGES

16. PRICE CODE

17. SECURITY CLASSIFICATION OF REPORT	18. SECURITY CLASSIFICATION	19. SECURITY CLASSIFICATION OF ABSTRACT	20. LIMITATION OF ABSTRACT
UNCLASSIFIED	UNCLASSIFIED	UNCLASSIFIED	UL

NSN 7540-01-280-5500

Standard Form 298 (Rev. 2-89)
Prescribed by ANSI Std Z39-18
298-102

FINAL REPORT

HETERODYNING SINGLE-PHOTON PAIRS*

OFFICE OF NAVAL RESEARCH AWARD NO. N00014-93-1-0547

MALVIN C. TEICH, PROFESSOR, PRINCIPAL INVESTIGATOR
COLUMBIA UNIVERSITY
NEW YORK, NEW YORK 10027

***PUBLICATIONS THAT RESULTED FROM SUPPORT BY THIS GRANT**

[1] A. Joobeur, B. E. A. Saleh, and M. C. Teich, "Spatiotemporal Coherence Properties of Entangled Light Beams Generated by Parametric Down-Conversion," *Phys. Rev. A* **50**, 3349-3361 (1994).

[2] T. S. Larchuk, M. C. Teich, and B. E. A. Saleh, "Statistics of Entangled-Photon Coincidences in Parametric Downconversion," *Ann. N.Y. Acad. Sci.* **755** (Fundamental Problems in Quantum Theory) 680-686 (1995).

[3] T. S. Larchuk, M. C. Teich, and B. E. A. Saleh, "Nonlocal Cancellation of Dispersive Broadening in Mach-Zehnder Interferometers," *Phys. Rev. A* **52**, 4145-4154 (1995).

[4] A. Joobeur, B. E. A. Saleh, T. S. Larchuk, and M. C. Teich, "Coherence Properties of Entangled Light Beams Generated by Parametric Down-Conversion: Theory and Experiment," *Phys. Rev. A* **53**, **in press** (1996).

Abstract: We have obtained theoretical and experimental second- and fourth-order interference patterns for entangled photons of different colors entering single and dual Mach-Zehnder interferometers (MZIs) in which dispersive elements have been deliberately placed.[1,2] Entangled-photon pairs are a form of nonclassical light. We have observed the interference of entangled photons of different colors, in both second- and fourth-order, using coincidence detection, by sweeping the path-length difference in an interferometer (or two spatially separated interferometers). The entangled photons are created by pumping a KD*P parametric-downconverter crystal with a krypton-ion laser beam at 413 nm, creating photon pairs with center wavelengths in the vicinity of 830 nm. The coherence properties and photon statistics of this nonclassical source of light were determined. Although photon wavepackets are generally broadened, as well as delayed, by passage through dispersive optical elements, coincidence measurements made with entangled photon pairs can be free of such broadening. This occurs for materials with particular dispersive behavior, as well as when the dispersion is balanced in both arms. This nonlocal behavior arises from the entanglement in the frequencies of the downconverted pair photons. We have shown that pump-frequency oscillations are present in the coincidence rate patterns for arbitrarily long path-length-difference times, confirming the robustness of this nonlocal phenomenon in the presence of dispersion. The difference-frequency oscillations, which correspond to heterodyning single-photon pairs, are also robust in the presence of dispersion, though they decay for large path-length-differences. Potential areas of applicability of twin photon beams range from photonics to visual science to computer science. Three examples are: (1) the direct measurement of the gain fluctuations in fiber amplifiers and avalanche photodiodes; (2) the direct determination of neural noise in a visual photoreceptor; and (3) key sharing in a quantum-cryptographic system for secure communications.

It is well known that the entangled nature (nonfactorizable state) of the photon pair produced in parametric downconversion results in a variety of nonlocal phenomena.[3] In an example recently discussed by Franson,[4] the two photons of the pair can be detected in coincidence even when they are passed through separate dispersive elements.

A schematic diagram of the configuration envisioned by Franson[4] for displaying this effect is shown in Fig. 1. Photons from a laser pump beam are converted into entangled photon pairs by spontaneous parametric downconversion in a $\chi^{(2)}$ nonlinear optical medium.[3-5] The photons of the entangled pair, created nearly simultaneously,[6] exit the nonlinear medium in what are traditionally called signal and idler beams. They travel through two dispersive optical elements, with thicknesses z_1 and z_2 which impart phase shifts to them, before reaching two photon detectors (labeled DET A and DET B in Fig. 1). The individual photon wavepackets are delayed and broadened in time by the dispersive elements in the same way that a classical electromagnetic pulse is broadened. Nevertheless, the photons remain coincident in the special case when their dispersion coefficients are equal in magnitude and opposite in sign.[4] This nonlocal behavior arises from the anticorrelation in the frequency components of the two photons, engendered by energy conservation.

Steinberg, Kwiat, and Chiao examined, both from a theoretical[7] and from an experimental[8] point of view, the case in which only one of the photons of a degenerate entangled photon pair traversed a dispersive medium of thickness z_1, imparting to the beam a phase shift. This photon was then interfered with its twin at a single beamsplitter before coincidence detection (see Fig. 2). Except for the dispersive element, this configuration is the same as that used by Hong, Ou, and Mandel[9] to demonstrate fourth-order interference at a beamsplitter. The effect is revealed by the

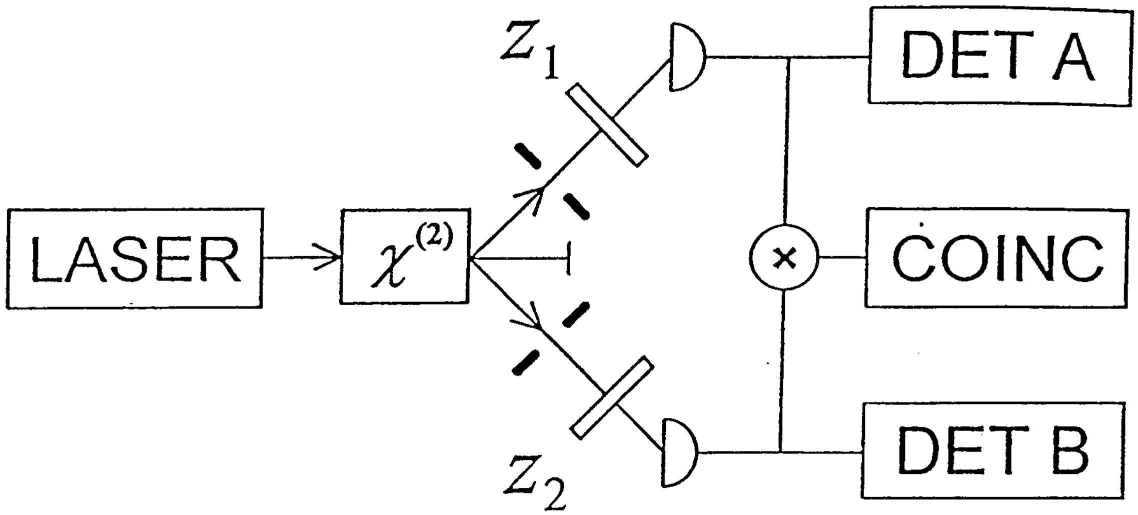

Figure 1. Schematic diagram of the configuration envisioned by Franson.[4] A pair of entangled photons, generated by spontaneous parametric downconversion in a $\chi^{(2)}$ nonlinear optical medium, pass through dispersive optical elements of thicknesses z_1 and z_2, which introduce phase shifts. Photon detectors A and B record the events in the signal and idler beams, respectively, and coincidence events are monitored. For particular selections of the dispersive media, the photons remain coincident.

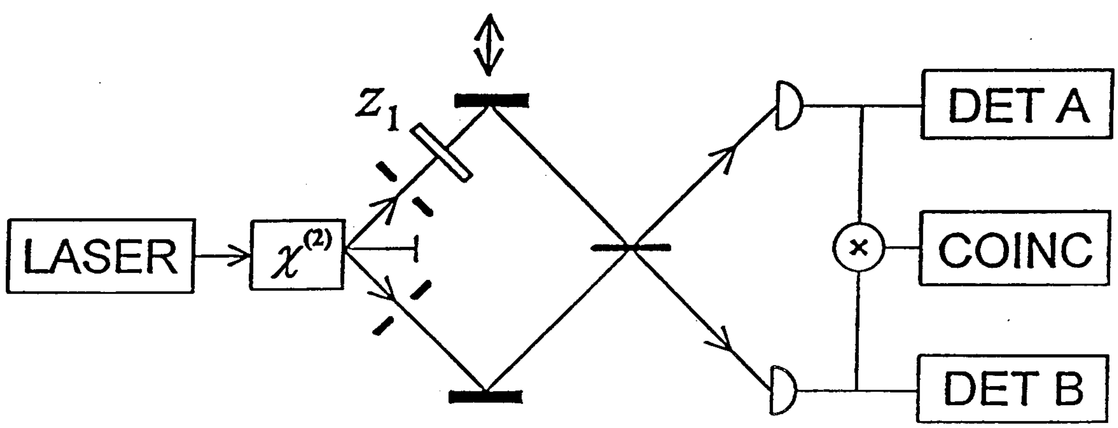

Figure 2. Schematic diagram of the configuration considered by Steinberg, Kwiat, and Chiao.[7,8] A dispersive element of thickness z_1, which introduces a frequency-dependent phase shift, is placed in one of the downconversion beams. This beam is also subjected to a variable path-length change relative to the other beam before they interfere in fourth-order at a beamsplitter. The narrow dip in the coincidence rate is not broadened by the presence of the dispersive element; its presence requires only that the centers of the wavepackets meet simultaneously in the beamsplitter.

presence of a narrow dip in the coincidence rate as one of the twin photons is delayed with respect to the other.[9,10] The coincidence dip reflects the tendency of two indistinguishable photons to stick together[11] (the dip can extend to zero only for degenerate photons). From a classical point of view dispersion would be expected to broaden the wavepackets, and therefore the dip, but entanglement renders the dip free of such broadening. The occurrence of the dip depends only on the centers of the wavepackets meeting simultaneously at the beamsplitter.[8] Thus, the sub-picosecond measurement resolution of arrival-time differences of pair photons at a fouth-order beamsplitter interferometer is not degraded by the presence of a dispersive element. Dispersive elements more complex than a simple glass plate lead to similar results.[12]

We have examined the behavior of second- and fourth-order interference patterns, and in particular the nonlocal character of the coincidence, at the output of a dispersive Mach-Zehnder interferometer on which downconverted beams are incident.[1] We considered two MZI configurations. The first, shown in Fig. 3(a), has the two beams overlapping fully within the interferometer (denoted full spatial overlap, FSO), whereas the second, shown in Fig. 3(b), has the two beams passing through the interferometer with no spatial overlap (NSO). This latter configuration is therefore equivalent to dual MZIs. Dispersive media with different thicknesses z_1 and z_2 add phase shifts to the optical beams traveling through the arms of the interferometer. The experimental arrangement is similar to that used in our earlier MZI measurements[13,14] except that dispersion is purposely introduced in these experiments.

The interference pattern is traced out by changing the path-length difference between the arms of the interferometer. This is effected by moving one of the interferometer mirrors (indicated by the double-sided arrows in Fig. 3). The output beams from the interferometer are directed to detectors A and B, as shown in Fig. 3. The events at the detector outputs are counted during a time of duration T, both marginally (in second-order), and as coincidences (in fourth-order), as a function of the path-length-difference time τ.

The theory detailing the effects of dispersion on the second- and fourth-order interference patterns has been reported in substantial detail and we will not repeat it here.[1] In this report, we concentrate on the experimental results that we have obtained using the experimental arrangement shown in Fig. 3.

Experiment

A Coherent Model 302 Krypton-ion laser, operated on the 413.1-nm violet line, served as the pump. An intracavity etalon insured that the laser operated on a single longitudinal mode, and the spatial aperture was adjusted to obtain $TEM_{0,0}$ transverse-mode operation. The optical power at the laser output was set at 100 mW and power stabilization and mode stabilization were activated.

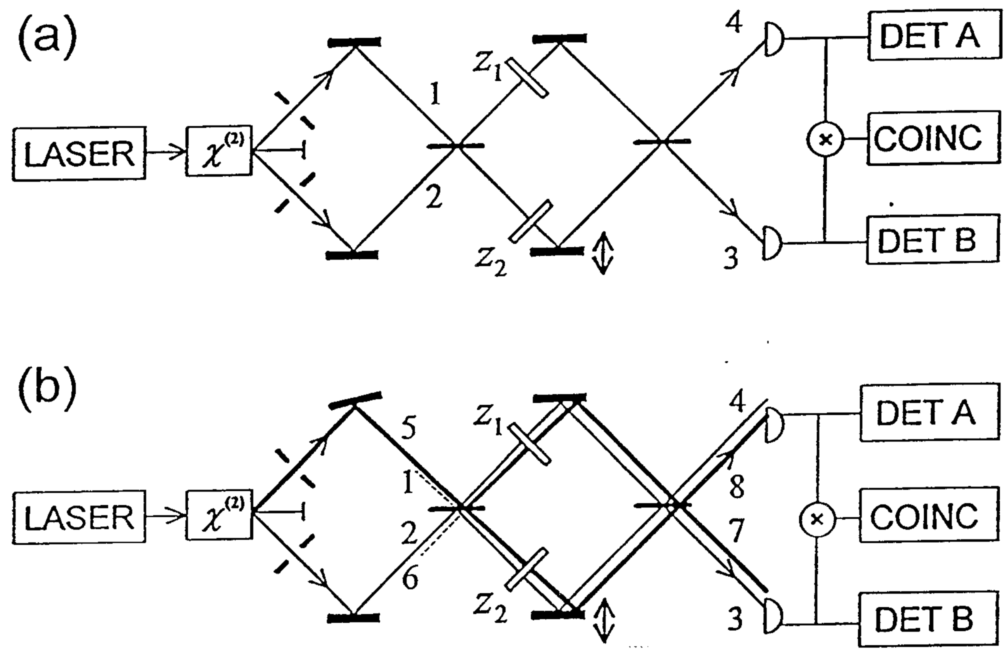

Figure 3. Schematic diagram of the MZI experiments considered here. Dispersive elements of thicknesses z_1 and z_2 are placed in one or both arms of the interferometer. The photons emerging from the ports of the interferometer are directed to photon detectors A and B. The detector output events are counted, both marginally and as coincidences, as the path-length-difference time τ is varied (by moving the mirror in the interferometer indicated with a double-edged arrow). Two MZI configurations were used:[1] (a) The two beams overlapped fully within the interferometer; this condition is denoted full spatial overlap (FSO). (b) The two beams passed through the interferometer with no spatial overlap; this is denoted NSO. The latter configuration was obtained by slightly rotating one of the mirrors that guides the light into the interferometer. It is equivalent to using two separate MZIs.

After attenuation by a neutral-density filter, approximately 1 mW of pump power was focused onto a 10-mm-long lithium iodate ($LiIO_3$) downconversion crystal oriented for type-I (ooe) phase matching, with the extraordinary-polarized pump incident at 42.8° to the optic axis of the crystal. Unconverted pump photons passed straight through the crystal and into a beam dump.

Downconverted photons emerge at an angle to the pump beam, with degenerate photons emerging symmetrically in a cone with a (external) half angle of about 9°, in most of our experiments; however, we used nondegenerate photons, which emerge asymmetrically in accordance with the energy- and phase-matching conditions. With apertures of about 2-mm diameter, we selected out desired nondegenerate photon pairs with center frequencies of about 813 and 840 nm. The statistics of the marginal and coincidence detections using this arrangement have been discussed previously.[15]

The photons were then directed, by mirrors, into the two input ports of the interferometer. The actual experiment made use of a folded Mach-Zehnder interferometer in which the beams were redirected onto a lower portion of the same beamsplitter cube by two retroreflectors. One of the retroreflectors was mounted on a movable translation stage used to change the path-length-difference time between the two interferometer arms. For the unbalanced-dispersion experiments, a 1/2-in-thick plate of BK7 glass was inserted into the movable arm of the interferometer (thus $z_2 = 2.54$ cm since the beam makes a double pass through the glass).

By adjusting the angle of one of the input mirrors, the photons' paths within the interferometer could be made to exhibit either FSO [Fig. 3(a)] or NSO [Fig. 3(b)]. For both types of experiments, the path length of only one arm of the interferometer was varied (by changing the position of the movable retroreflector).

The photons exiting the interferometer were passed through focusing lenses and a pair of RG-695 filters to block the pump light, and then allowed to impinge onto two custom-configured single-photon counting modules (RCA type SPCM-100; now sold by EG&G). At the heart of these detectors lie passively-quenched avalanche photodiodes whose diameter for peak photon-detection efficiency is about 100 μm.

After suitable compensation for electronic delay differences, the signals from the two-photon-counting modules were sent to a pair of Berkeley Nucleonics Corp. type 8010 pulse-generators that produced standardized 10-ns wide pulses triggered by the leading edges of the detector-module outputs. These standardized pulses were then sent to the dual inputs of a Stanford Research Systems type SR400 Two-Channel Gated Photon Counter and counted for 1 s to provide a measure of the rate of photon detections at each of the output ports. They were also added together and sent to a Hewlett-Packard type 5370A Universal Time-Interval Counter which, triggered by the gated photon counter, counted for 1 s to provide a measure of the coincidence rate.

The interference patterns for unbalanced dispersion, with $z_2 = 2.54$ cm and $z_1 = 0$, are presented in Figs. 4 and 5 for FSO and NSO, respectively. The upper panels show the counts recorded by detector B (at output port 3), the middle panels show the counts recorded by detector A (at output port 4 for FSO and output port 8 for NSO), and the lower panels show the coincidence counts (at output ports 3 and 4 for FSO and at output posts 3 and 8 for NSO). The black data points fill out the envelopes of the interference patterns but do not have the resolution to trace out the harmonic variation at the scale of the figure. All of the data in each figure were collected in the same experimental run.

The data in Figs. 4 and 5 may be compared with the theoretical results presented in Ref. 1. Satisfactory fits to the data in Fig. 4 for FSO, shown as gray dots, were obtained by using Eqs. (5'), (6'), and (8') in [1] with the values $V_3 = V_4 = V_{34} = 0.7$, $N_3 = 29684$, $N_4 = 29088$, and $N_{34} = 475.96$. Satisfactory fits to the data in Fig. 5 for NSO, also shown as gray dots, were

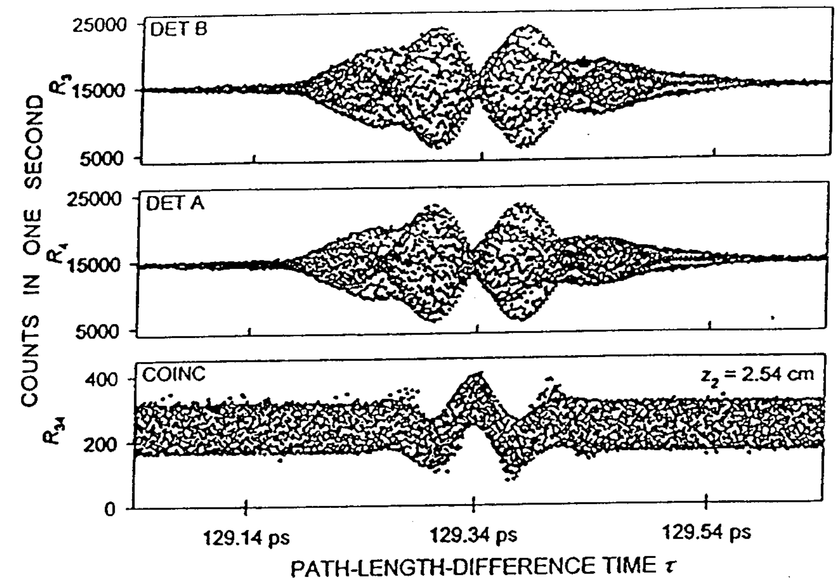

Figure 4. Mach-Zehnder interference patterns for unbalanced dispersion with full spatial overlap (FSO). Experimental data (black dots) and theoretical results (gray dots) with $z_2 = 2.54$ cm of BK7 glass inserted in one arm of the interferometer ($z_1 = 0$). The upper panel shows the counts recorded by detector B, the middle panel shows the counts recorded by detector A, and the lower panel shows the counts recorded in coincidence between detectors A and B. The vertical scale represents the number of counts recorded in one second for each path-length-difference time τ (corresponding to a different position of the retroreflector).

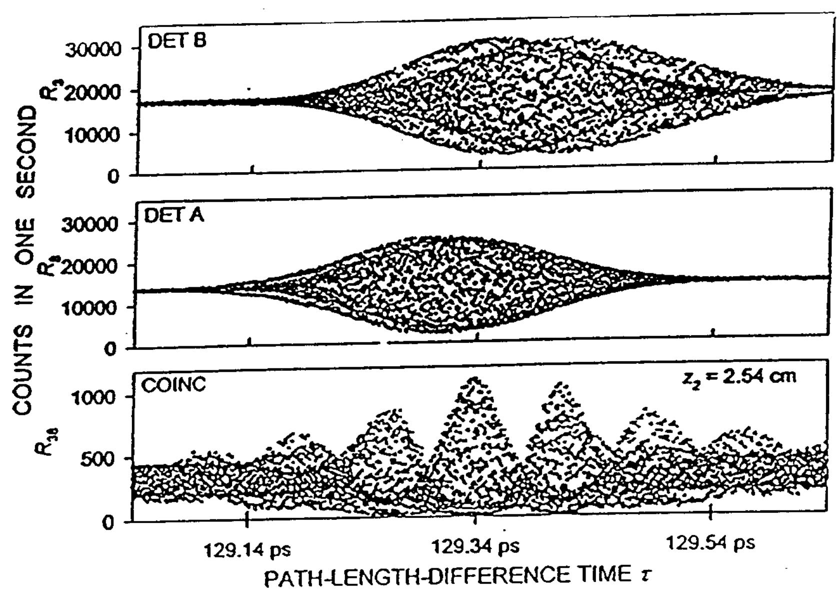

Figure 5. Mach-Zehnder interference patterns for unbalanced dispersion with no spatial overlap (NSO). Experimental data (black dots) and theoretical results (gray dots) with $z_2 = 2.54$ cm of BK7 glass inserted in one arm of the interferometer ($z_1 = 0$). The upper panel shows the counts recorded by detector B, the middle panel shows the counts recorded by detector A, and the lower panel shows the counts recorded in coincidence between detectors A and B. The vertical scale represents the number of counts recorded in one second for each path-length-difference time τ (corresponding to a different position of the retroreflector).

obtained by using Eqs. (11'), (12'), and (13') in [1] with the values $V_3 = V_8 = 0.8$, $V_{38} = 0.85$, $N_3 = 33904$, $N_8 = 27628$, and $N_{38} = 1258.89$. In both cases we chose $\lambda_p = 413.1$ nm, $\lambda_1 = 840.0$ nm, $\lambda_2 = 813.8$ nm, and $\sigma = 1.25 \times 10^{13}$ s^{-1}. The values of β_0, β_1, and β_2 are provided in Ref. 1.

Though the fits of the data to the theory are reasonable, they are not perfect. The lack of agreement is not unexpected because of the idealized nature of the simple joint-Gaussian state used for the calculations presented here. We have determined that the fits can be substantially improved by incorporating additional phenomenological parameters in the equations. In fact, a more thorough treatment of the downconversion process that accounts for finite pump-beam waist, pump spectral width, and crystal length, yields a state that does contain additional parameters.[2, 16] The interference patterns obtained by using this more sophisticated description are substantially more complex than those presented here and are expected to provide a superior match with the experimental results.

Conclusion

A variety of unusual fourth-order interference patterns emerge when nondegenerate entangled photon pairs are fed into single and dual Mach-Zehnder interferometers in which dispersive elements have been deliberately placed.

The singles rates, reflecting second-order interference, are affected by dispersion in the usual manner expected for classical fields. However, the anticorrelation in the frequencies of the downconverted pair photons give rise to nonlocal behavior that can, under certain conditions, allow the cancellation of dispersive broadening in the coincidence rate, reflecting fourth-order interference. Complete cancellation occurs for dispersive materials that obey $\beta_1(\omega_1) = \beta_1(\omega_2)$ and $\beta_2(\omega_1) = -\beta_2(\omega_2)$. In this case, the second- and fourth-order interference patterns are the same as those obtained in the nondispersive case. Although they decay, the difference frequency oscillations are highly robust.

Many fourth-order interference experiments carried out previously, using both degenerate and nondegenerate photon pairs, have revealed the existence of nonlocal pump-frequency oscillations in the coincidence rate that continue for large path-length-difference times. We have shown, both theoretically and experimentally, that these oscillations persist in the presence of dispersion, though in general their visibility is reduced. However, for unbalanced dispersion, using materials that possess the special characteristics $\beta_1(\omega_1) = \beta_1(\omega_2)$ and $\beta_2(\omega_1) = -\beta_2(\omega_2)$, and for balanced dispersion, the pump-frequency oscillations have precisely the same visibility as they do in the absence of dispersion.

References

1. T. S. Larchuk, M. C. Teich, and B. E. A. Saleh, Phys. Rev. A 52, 4145 (1995).
2. A. Joobeur, B. E. A. Saleh, T. S. Larchuk, and M. C. Teich, "Coherence Properties of Entangled Light Beams Generated by Parametric Downconversion: Theory and Experiment," Phys. Rev. A in press (1996).
3. J. Peřina, Z. Hradil, and B. Jurčo, *Quantum Optics and Fundamentals of Physics* (Kluwer, Boston, 1994).
4. J. D. Franson, Phys. Rev. A 45, 3126 (1992).
5. D. C. Burnham and D. L. Weinberg, Phys. Rev. Lett. 25, 84 (1970).
6. S. Friberg, C. K. Hong, and L. Mandel, Phys. Rev. Lett. 54, 2011 (1985).
7. A. M. Steinberg, P. G. Kwiat, and R. Y. Chiao, Phys. Rev. A 45, 6659 (1992).
8. A. M. Steinberg, P. G. Kwiat, and R. Y. Chiao, Phys. Rev. Lett. 68, 2421 (1992).
9. C. K. Hong, Z. Y. Ou, and L. Mandel, Phys. Rev. Lett. 59, 2044 (1987).
10. J. G. Rarity, Ann. N.Y. Acad. Sci. 755, 624 (1995).
11. R. A. Campos, B. E. A. Saleh, and M. C. Teich, Phys. Rev. A 42, 4127 (1990).
12. G. S. Agarwal and S. D. Gupta, Phys. Rev. A 49, 3954 (1994).
13. T. S. Larchuk, R. A. Campos, J. G. Rarity, P. R. Tapster, E. Jakeman, B. E. A. Saleh, and M. C. Teich, Phys. Rev. Lett. 70, 1603 (1993).
14. J. G. Rarity, P. R. Tapster, E. Jakeman, T. S. Larchuk, R. A. Campos, M. C. Teich, and B. E. A. Saleh, Phys. Rev. Lett. 65, 1348 (1990).
15. T. S. Larchuk, M. C. Teich, and B. E. A. Saleh, Ann. N. Y. Acad. Sci. 755, 680 (1995).
16. A. Joobeur, B. E. A. Saleh, and M. C. Teich, Phys. Rev. A 50, 3349 (1994).